Polymorphism, Pseudo-polymorphism, and Conformerism in the Crystal Structure of Piperazine-N,N'-bis(N, O-diphenyl phosphoramidate) †

Khodayar Gholivand,*[a] Mahdieh Hosseini,[a] Ali A. Ebrahimi Valmoozi, [a] Kaveh Farshadfar,[a]

[a] Department of Chemistry, Faculty of Science, *Tarbiat Modares University*, Tehran, Iran

Electronic Supplementary Information†

Experimental Section

General

All chemicals and solvents used in the syntheses were commercially available and were used without further purification. ^{1}H, ^{31}P, and ^{13}C NMR spectra were recorded on a Bruker Avance DRX500 MHz NMR spectrometer. IR spectrum was recorded on a Nicolet 510P spectrophotometer using KBr disks

Synthesis of Piperazine -N,N'-bis (N,O-diphenyl phosphoramidate), L_{OphAn}

$(C_6H_5O)(C_6H_5NH)P(O)Cl$ was prepared by the reaction of Aniline with $(C_6H_5O)P(O)Cl_2$ in 2: 1 molar ratio. Aniline was added dropwise to a CH_3CN solution (20 ml) of $(C_6H_5O)P(O)Cl_2$ at 0 C. After 4 hours stirring, the solvent was removed in vacuum and the resulting was washed with distilled water and dried.

The compound, L_{OPhAn} was synthesized by the reaction of 2mmol of $(C_6H_5O)(C_6H_5NH)P(O)Cl$ and one mmol of piperazine in the presence of Et_3N as HCl scavenger in CH_2Cl_2 at room temperature. After stirring for 24 h, the solvent was evaporated and the residue was washed with distilled water and dried. Physical and spectroscopic data of L_{OPhAn} are presented below:

FT-IR (KBr pellet, cm^{-1}): 2916.2 (s), 1597.5 (s), 1492.4 (s), 1222.0 (P=O), 1117.6 (P–O), 928.9 (s), 754.8 (P–N). m.p. 243 °C. ^{1}H NMR (500.13 MHz, d6–DMSO, 25°C, TMS); δ= 2.79–2.94 (m, 8 H, CH_2), 6.85–6.89 (m, 2 H, Ar), 7.02–7.03 (m, 4 H, Ar), 7.11–7.20 (m, 8 H, Ar), 7.33–7.36 (m, 6 H, Ar), 8.06 (2 H, $^{2}J_{PNH}$ = 9.3 Hz, 2 H, NHC_6H_5) ppm. ^{13}CNMR (125.75 MHz, d6–DMSO, 25°C, TMS); δ= 43.93 (d, $^{2}J_{PC}$ = 3.5 Hz, 4 C, CH_2), 117.56 (m, 4 C, ortho–HNC_6H_5), 120.35 (m, 2 C, para–HNC_6H_5), 120.80 (m, 4 C, ortho–OC_6H_5), 124.48 (m, 2 C, para–OC_6H_5), 128.90 (m, 4 C, meta–OC_6H_5), 129.66 (m, 4 C, meta–HNC_6H_5), 140.74 (s, 2 C, ipso–HNC_6H_5), 150.48 (d, ^{2}JPC = 5.7 Hz, 2 C, ipso–OC_6H_5) ppm.$^{31}P\{1H\}$ and ^{31}P NMR (202.45 MHz, d6–DMSO, 25°C, H_3PO_4 external); δ= 4.51 (m) ppm.

Crystal structure determination

X-ray data of compounds were collected methods and refined by full-matrix least squares methods against F^2 in anisotropic approximation (for non-H atoms) using SHELXL97[1] for forms I and III and SHELXTL[2] for Form II.MeOH. For I and III, The H(C) atom positions were calculated, and they were refined in isotropic the approximation in riding model with the $U_{iso}(H)$ parameters equal to 1.2 $U_{eq}(C_i)$, where $U(C_i)$ are respectively the equivalent thermal parameters of the carbon atoms to which the corresponding H atoms are bonded. The positions of H(N) atoms were located from the Fourier density synthesis and refined in the isotropic approximation. For II.MeOH, The H atoms of the NH and OH groups were localized in the difference Fourier-syntheses. The H(C) atoms were placed in calculated positions. All hydrogen atoms were included in the refinement within riding model with fixed isotropic displacement parameters ($U_{iso}(H)$ = 1.2U_{eq}(C, N, O)). Structural illustrations have been drawn with MERCURY.[3] The Crystallographic and refinement data are summarized in Table S1. Independent part of the unit cell which contains the minor component of the disordered atoms of II.MeOH is shown in Figure S1.

Results and discussion

Table S1. Crystal Data and Structural Refinement for Compounds I, II.MeOH and III

	(I)	**(II**. MeOH**)**	**(III)**
formula	C28 H30 N4 O4 P2	C28 H30 N4 O4 P2, 2(C H4O)	C28 H30 N4 O4 P2
fw	548.50	612.58	548.50
λ/Å	0.71073	0.71073	0.71073
T/K	150(2)	100(2)	100(2)
crystal.system	Monoclinic	Monoclinic	Orthorhombic
space group	$P2_1/c$	$P2_1/c$	$P\ 2_1\ 2_1\ 2_1$
a/Å	9.422(3)	10.4656(4)	12.9321(4)
b/Å	10.045(3)	13.8598(5)	19.0714(6)
c/Å	14.165(4)	11.2698(4)	21.9285(7)
α/°	90	90	90
β/°	94.264(5)	110.7680(10)	90
γ/°	90	90	90
V/Å^3	1336.9(6)	1528.48(10)	5408.3(3)
D_{calc}/Mg m^{-3}	1.363	1.331	1.347
Z	2	2	8
μ/mm^{-1}	0.205	0.191	0.203
F(000)	576	648	2304
2θ/°	58	60	58
R(int)	0.0372	0.0288	0.0212
GOOF	0.968	1.050	1.065
R_1(I > 2σ(I))	0.0427	0.0491	0.0320
wR_2(I > 2σ(I))	0.1029	0.1184	0.0844
CCDC No.	1027076	1424112	1027078

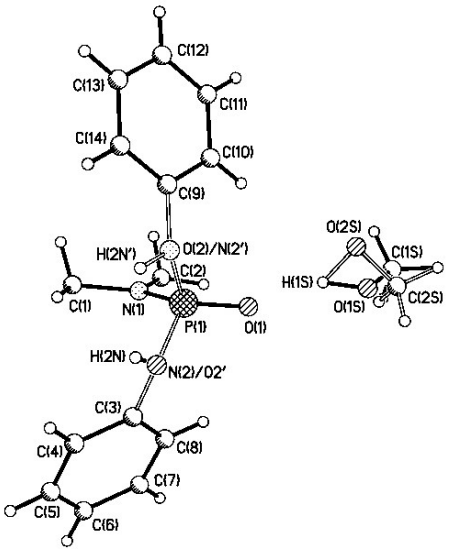

Figure S1. Independent part of the II.MeOH unit cell. The methanol solvate molecule is disordered over two positions with 0.67/0.33 occupancies. N(2)H group and O(2) atom are also disordered over two positions with 0.67/0.33 occupancies.

The Cambridge Structural Database (CSD) analysis for describing conformational features of phosphoramidates.

The Cambridge Structural Database (CSD) analysis for the investigation of the conformational behavior of phosphoramide compounds was carried out using CSD, version 5.38, November 2016 update. The search was based on the fragment shown in Fig. S2(a). 43 hits were found and the different torsion angles of these molecules were defined. The two-step clustering analysis, performed with IBM SPSS Statistics 24.0, was used for the classifying the torsion angles of different molecules. First, molecules were clustered based on θ_1 and θ_2 (clustering No.1) and then θ_3 and θ_4 (clustering No.2). The Refcodes, torsion angles of CSD search and cluster membership of each molecule are shown in Table S2. Distributions of the clusters for clustering **1** and clustering **2** are shown in Table S3. Refcodes and X-ray geometrical parameters of intramolecular interactions involved in the third cluster of clustering **2**, are shown in Table S4.

Table S2 Refcodes, determined θ_1- θ_5 and the clustering membership of the molecules found searching CSD and I, II, III-A and III-B.

Refcode	NPNC(θ_1)	OPNC(θ_2)	NPOC(θ_3)	OPOC(θ_4)	CN^OC(θ_5)	Clustering 1 Membership	Clustering 2 Membership
AWUFOO	76.29	48.01	70.24	49.96	15.65	3	2
CEPSEV	50.25	76.21	162.33	73.99	174.27	3	1
CEQBEG	54.72	73.29	157.57	78.02	176.28	3	1
CEQBIK (A)	48.73	79.17	160.1	73.48	176.65	3	1
CEQBIK (B)	50.14	77.6	160.14	72.74	178.19	3	1
DEZSOQ	45.62	84.02	163.46	68.54	176.95	3	1
EDEXAO (A)	157.87	28.53	90.86	42.76	85.72	2	-
EDEXAO (B)	162.53	32.39	88.43	45.37	93.77	2	-
ERUFIH	39.15	170.92	173.32	46.42	109.56	1	1
EXISIO	168.78	64.18	58.2	179.66	85.04	2	3
GEPMEU	179.33	57.67	79.95	43.06	101.62	2	2
GUDGOC	67.74	57.98	173.91	64.3	136.66	3	1
LIGRUO	131.96	0.34	154.67	25.74	22.99	2	1
MEKSIE (A)	24.07	149.5	141.33	16.99	147.65	1	1
MEKSIE(B)	33.47	159.16	142.09	17.86	142.55	1	1
MUBPIJ	55.89	69.47	79.6	40.6	70.44	3	2
NANROJ	68.66	56.12	168.81	45.65	119.07	3	1
NANROP	167.42	41.92	43.97	173.76	108.84	2	3
NIBPAQ	169.89	44.19	53.43	177.55	97.66	2	3
OCAVIZ	40.32	170.63	175.9	51.62	102.96	1	1
OXPOTU (A)	37.91	171.07	79.23	49.94	166.37	1	-
OXPOTU (B)	38.09	169.76	41	84.73	51.35	1	-
OXPOTU01 (A)	38.84	169.8	40.83	83.73	53.98	1	-
OXPOTU01 (B)	39.11	170.51	75.09	50.52	159.83	1	-
PECNOC (A)	69.73	56.2	144.88	24.07	112.18	3	-
PECNOC (B)	148.16	17.8	178.24	56.22	20.46	2	-
PECNOC01	80.13	45.61	81.11	40.76	5.01	3	-
PECSIZ	77.19	49.18	30.75	153.55	145.32	3	3

PECSOF	75.26	51.08	31.26	154.1	139.41	3	3
PECSUL	55.85	175.64	46.22	81.56	101.08	1	2
QIBBAF	119.94	114.37	159.8	76.28	34.79	3	1
QIQJOR	75.66	52.28	58.07	67.55	58.49	3	2
QIQJUX	178.26	55.32	75.63	48.32	106.6	2	2
RISCIF (A)	28.59	156	116.09	8.16	168.37	1	1
RISCIF (B)	29.18	156.32	119.68	3.29	166.05	1	1
SACVOI	179.55	54.92	79.59	43.54	97.13	2	2
SACYEA	168.14	66.73	50.23	179.53	86.98	2	3
SOYBUD (A)	55.64	71.36	161.69	74.96	169.42	3	1
SOYBUD (B)	45.91	82.17	53.87	71.19	120.76	3	2
SOYCAK	62.06	64.59	162.78	75.17	155.23	3	1
TASQIN	67.33	58.89	154.94	33.07	121.78	3	1
TEGDAK	51.57	176.51	157.59	81.35	73.37	1	1
VABBOQ (A)	11.62	139.23	143.48	18.86	154.22	1	1
VABBOQ (B)	44.11	172.21	174.63	50.77	109.77	1	1
VABBUW	17.7	145.93	146.72	22.34	149.75	1	1
VABCAD (A)	44.09	173.74	179.12	54.5	105.12	1	1
VABCAD (B)	4.3	133.43	141.95	17.13	162.25	1	1
VORVAB	172.52	44.46	78.67	51.11	110.08	2	2
YUPVEL	49.18	75.73	60.38	62.77	18.2	3	2
ZUFPEV	31.22	159.85	145.95	21.72	140.52	1	1
ZUFPOF (A)	44.82	170.95	169.08	45.73	117.28	1	1
ZUFPOF (B)	38.09	164.45	169.82	46.84	121.49	1	1
I	63.4	63.2	171.4	48.6	136.4	3	1
II	39.9	85.2	49.8	75.6	12.7	3	2
III-A(up)	62	63.5	165.7	42.9	137.7	3	1
III-A(down)	58.1	68.1	170.5	47.5	154.5	3	1
III-B(up)	68.2	58	176.5	62.4	139.2	3	1
III-B(down)	57.4	68.8	46	78.2	16.9	3	2

Table S3 Clustering No.1 and 2; clusters distribution

	cluster	N	% of Combined	% of Total
Clustering (No.1)	1	20	34.5%	34.5%
	2	12	20.7%	20.7%
	3	26	44.8%	44.8%
	Combined	58	100.0%	100.0%
Total		**58**		**100.0%**
Clustering (No.2)	1	31	63.3%	63.3%
	2	12	24.5%	24.5%
	3	6	12.2%	12.2%
	Combined	49	100.0%	100.0%
Total		**49**		**100.0%**

TableS4 Refcodes and X-ray geometrical parameters of intramolecular interactions involved in the third cluster of clustering **2.**

Refcode	Involved intramolecular interactions	HB Graph set	X-ray Geometry (Å/deg)*
AWUFOO	$CH_{OPh}\cdots\pi_{central\ amine}$	---	3.515/154
GEPMEU	$C\text{-}H_{OR}\cdots O_{P=O}$	$S_1^1(5)$	2.803/2.999(3)/91
MUBPIJ	$CH_{OPh}\cdots\pi_{central\ amine}$	---	3.684/153
PECSUL	Cyclic OR group	---	---
QIQJOR	$CH_{OPh}\cdots\pi_{central\ amine}$	---	3.507/152
QIQJUX	$CH_{OPh}\cdots\pi_{central\ amine}$	---	2.889/150
SOYBUD(B)	Cyclic OR group	---	---
SACVOI	$C\text{-}H_{OR}\cdots O_{P=O}$	$S_1^1(5)$	2.557(4)/3.050(4)/106.8(3)
VORVAB	$CH\cdots\pi_{OPh}$	---	2.644/153
YUPVEL	$C\text{-}H_{OPh}\cdots O_{P=O}$	$S_1^1(6)$	2.518/3.167(2)/127
II	$C\text{-}H_{OPh}\cdots O_{P=O}$	$S_1^1(6)$	2.675/3.323(2)/126
III-B (down)	$C\text{-}H_{OPh}\cdots O_{P=O}$	$S_1^1(6)$	2.721/3.287(2)/119

* Geometrical parameters of HB-**bond**: H···A/ D···A/<D-H···A, **C-H···π**: CH···Cg/ C-H-Cg

The Cambridge Structural Database (CSD) analysis of CH···π contact in phosphoramide compounds

The CH···π contacts of CSD searched molecules based on the fragment shown in Fig.S2 (a) have been analyzed. The searches based on geometrical parameters of the H···Cg contact distance, C-H···Cg for CH···π interactions of phosphoramide compounds are shown in Figures S2 (b) and (c). Based on the contact distance histogram, most of the CH···π distances in three polymorphs are near the relative maximum in the number of examples around 3.2 to 3.8 Å. Moreover, the CH···π angle histogram shows that the most molecules lie between 125 to 165°, but the relative maximum number of examples is between 125 to 140°. For three polymorphs the CH···π angle values lie in a normal range. The Scatter-gram for a correlation between H···Cg distance/C-H···Cg angle is depicted in Figure S3. Compounds reported here are approximately around themaximum distribution area in this scatter-gram.

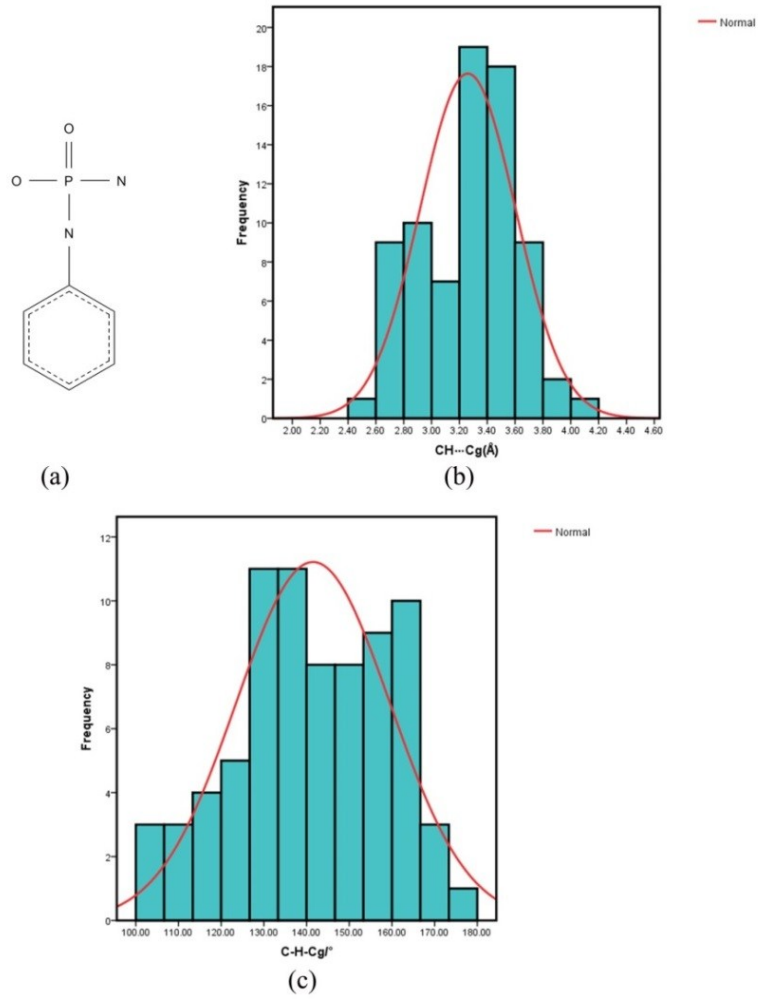

Figure S2. (a) A diagram of the molecular fragment used in the CSD search for exploring the conformational behavior and CH··· π contact in phosphoramide compounds. Histograms for the (b) H···Cg contact distance and c) C-H···Cg angle from the CSD search (43 hits containing 79 distinct CH···π contacts).

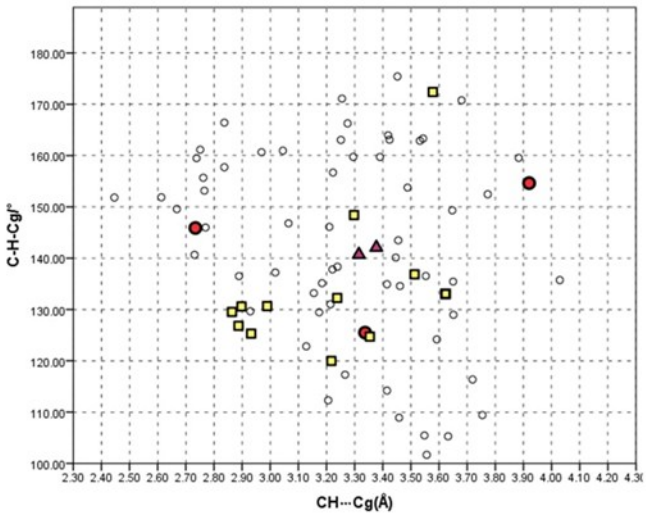

Figure S3. The Scattergrams for a correlation between CH···π contact distance and angle**.** The violet triangles, red circles and yellow squares are related to CH···π interactions in I, II and III, respectively.

The Cambridge Structural Database (CSD) analysis of P=O···NH hydrogen bonding in phosphoramide compounds

Furthermore, for comparing the P=O···H-N hydrogen bonding distance in II and III with the other phosphoramide compounds, a CSD search based on this intermolecular interaction was carried out. 110 hits, including 169 distinctive P=O···NH hydrogen bond distance were found. The search based on the H···O distance, is shown in Fig S4. The distance values of P=O···NH hydrogen bonding in I and III lie in a normal range in the maximum number of examples bins.

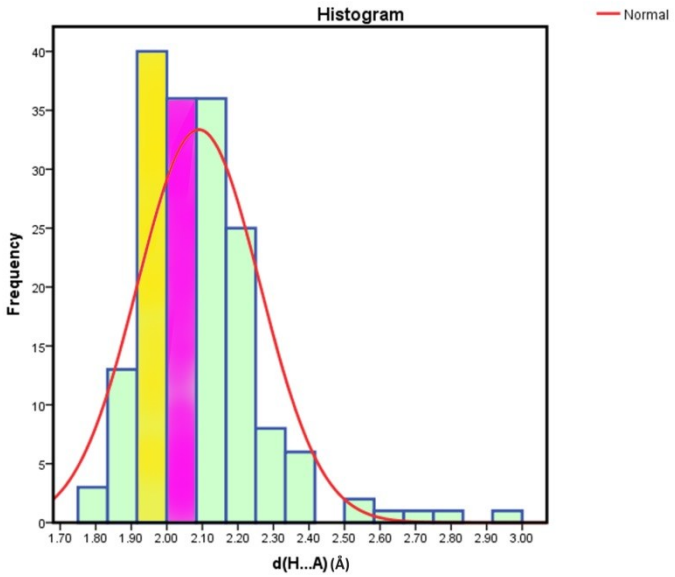

Figure S4. Histograms for the distance between the hydrogen atom of NH and oxygen atom of P=O groups from a CSD search. I and III are shown by violet and yellow columns, respectively.

Computational study details

Potential energy (E_p) of isolated molecule L_{OPhAn} in different conformations as a function of torsion C-N^O-C was calculated. For this purpose, torsion angle C-O^N-C was changed in 10 steps from 6 to 176°. In each step the mentioned torsion was frozen and the rest of the molecule was optimized by the MP2[4] approach and 6-311G basis set using Gaussian 09[5] program.

The potential energy of different conformers in the gas phase was calculated separately. For this purpose, the hydrogen atoms of the molecule were optimized and the rest of molecules were frozen by the MP2 approach and 6-311G basis set using Gaussian 09 program.

For NCI calculations, the considered structures were cut out directly from the CIF data and the hydrogen atoms of the molecules were optimized at the B3LYP/6-311G** level. NCI technique was carried out through the analysis of the reduced density gradient (RDG) with low densities[6] at the M062X/6-311+G** level using the Gaussian 09 package and Multiwfn program.[7] For this, The calculated grid points were plotted for a defined real space function, $sign(\lambda_2(r))\rho(r)$ and reduced density gradient (RDG) And a visualization of the gradient isosurface was depicted using the VMD 1.9.2 software.[8] The color of the isosurfaces is decided based on the value of $sign(\lambda_2)\rho$. Blue, green and red color codes are commonly used to describe stabilizing H-bonding, van der Waals and steric interaction, respectively. The pictures were provided for an isosurface value of s = 0.5.

Lattice energy of polymorph I, II.MeOH and III were calculated using the Forcite module of Material Studio 6 with COMPASS force field.[9] The Ewald summation employed to compute the non-bonded interactions that include van der Waals and electrostatic interactions. Finally, lattice energies were computed per molecule based on the number of molecules present in the unit cell

Hirshfeld surface analysis

the Hirshfeld surfaces and 2D fingerprint plots were produced by crystal explorer 3.1.[10] according to Crystallographic Information Files. It should be explained that for crystal structures where the molecule does not stand on a centre of inversion, intermolecular contacts are different for each side of the molecules. So in Figure 9, the Hirshfeld surfaces of Form III molecules are shown in two views labeled front and back.

Powder X-ray diffraction

X-ray powder diffraction (XRD) measurements were performed using a X'pert Pro MPD diffractometer with monochromated Cu-kα radiation (λ=1.54056Å). The simulated XRD powder pattern based on single crystal data was prepared using Mercury software.

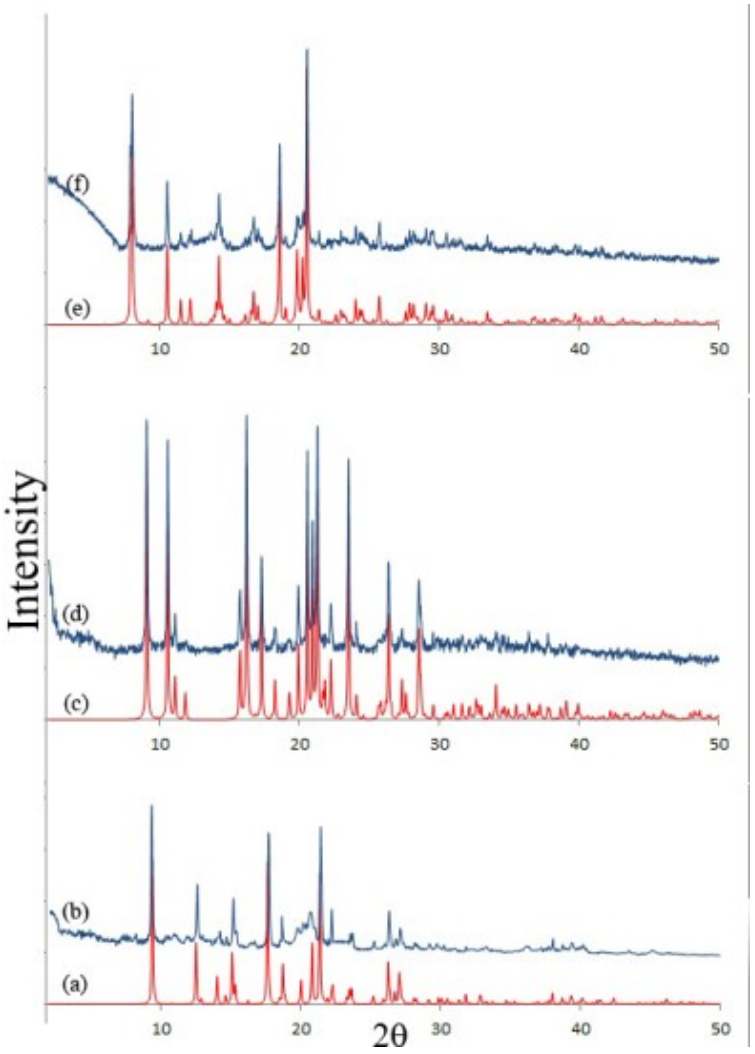

Figure S5. The simulated PXRD pattern of polymorphs I calculated from single-crystal data; b) experimental X-ray powder diagram of polymorph I; (c) simulated PXRD pattern of polymorph II.MeOH;(d) experimental X-ray powder diagram of polymorph II.MeOH; (e) simulated PXRD pattern of polymorph III; and (f) experimental X-ray powder diagram of polymorphs III.

FT-IR spectroscopy

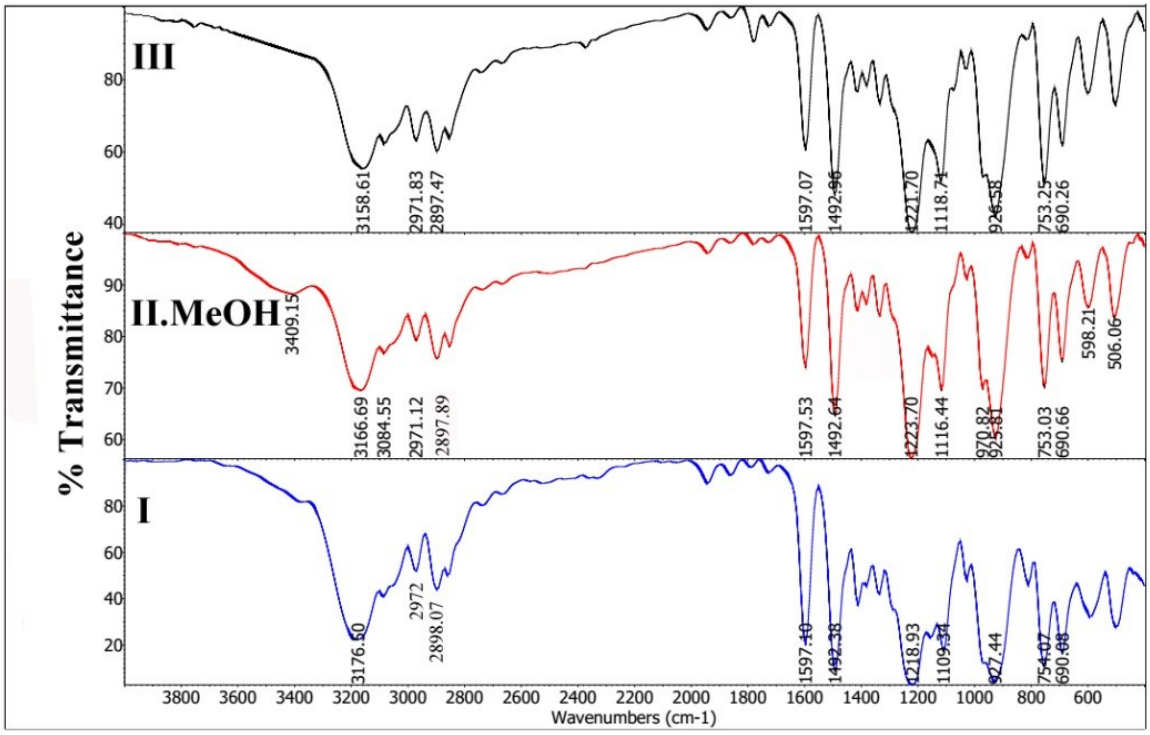

figure S6. FT-IR of I, II.MeOH and III.

Table S5. Vibrational frequency of polymorphs

FT-IR(Cm^{-1})	N-H stretch	C-H stretch	P=O stretch	P-O stretch	P-N
I	3176.50	2972.8	1218.93	1109.34	927.44
II.MeOH	3166.69	2971.12	1223.70	1116.44	925.44
III	3158.61	2971.83	1221.70	1118.71	926.55

Table S6. Selected bond distances in the crystal structure of I, II.MeOH and III.

Compound	N-H bond distance(Å)	P=O···NH hydrogen bond distance(Å)	P=O bond distance(Å)
I	0.84(3)	2.12(3)	1.472(1)
II.MeOH	0.881	---	1.470(1)
III	0.86(2); 0.98(2); 0.89(2); 0.91(2)	1.98(2); 1.931(19); 1.98(2); 1.941(19)	1.474(1); 1.471(1); 1.476(1); 1.478(1)

Thermal analysis

DSC was performed on a Mettler Toledo DSC 822e module. Samples were placed in crimped but vented aluminum sample pans. The temperature range was 30–300°C at a heating rate of 5°C/min.

References

1 Sheldrick, G., SHELX-97: Programs for crystal structure analysis. Göttingen, Germany, 1997.

2 Sheldrick, G. Acta Crystallogr. Sect. A., 2008, 64, 112.

3 Macrae, C. F.; Bruno, I. J.; Chisholm, J. A.; Edgington, P. R.; McCabe, P.; Pidcock, E.; Rodriguez-Monge, L.; Taylor, R.; van de Streek, J.; Wood, P. A. J. Appl. Crystallogr., 2008, 41, 466.

4 Head-Gordon, M.; Head-Gordon, T. Chem. Phys. Lett., 1994, 220, 122.

5 M.J. Frisch, G. W. T., H.B. Schlegel, G.E. Scuseria, M.A.; Robb, J. R. C., G. Scalmani, V. Barone, B. Mennucci,; G.A. Petersson, H. N., M. Cari- cato, X. Li, H.P.; Hratchian, A. F. I., J. Bloino, G. Zheng, J.L. Sonnenberg,; M. Hada, M. E., K. Toyota, R. Fukuda, J. Hasegawa, M.; Ishida, T. N., Y. Honda, O. Kitao, H. Nakai, T. Vreven,; J.A. Montgomery, J., J.E. Peralta, F. Ogliaro, M. Bearpark, J.J.; Heyd, E. B., K.N. Kudin, V.N. Staroverov, R. Kobayashi,; J. Normand, K. R., A. Rendell, J.C. Burant, S.S.; Iyengar, J. T., M. Cossi, N. Rega, J.M. Millam, M. Klene,; J.E. Knox, J. B. C., V. Bakken, C. Adamo, J. Jaramillo, R.; Gomperts, R. E. S., O. Yazyev, A.J. Austin, R. Cammi,; C. Pomelli, J. W. O., R.L. Martin, K. Morokuma, V.G.; Zakrzewski, G. A. V., P. Salvador, J.J. Dannenberg, S.; Dapprich, A. D. D., Ö. Farkas, J.B. Foresman, J.V. Ortiz, J.; Fox, C. a. D. J., Gaussian 09, Revision D.01, Gaussian. Inc., Wallingford, CT 2009.

6 Johnson, E. R.; Keinan, S.; Mori-Sánchez, P.; Contreras-García, J.; Cohen, A. J.; Yang, W. J. Am. Chem. Soc., 2010, 132, 6498.

7 Lu, T.; Chen, F. J. Comput. Chem., 2012, 33, 580.

8 Reed, A. E.; Curtiss, L. A.; Weinhold, F. Chem. Rev., 1988, 88, 899.

9 H. Sun. J. Phys. Chem. B., 1998, 102, 7338.

10 S. K. Wolff, D. J. Grimwood, J. J. McKinnon, M. J. Turner, D. Jayatilaka and M. A. Spackman, CrystalExplorer 3.0, University of Western Australia, Perth, Australia, 2012.